JACS
JOURNAL OF THE AMERICAN CHEMICAL SOCIETY

ARTICLE

pubs.acs.org/JACS

Formation of Aromatic Structures from Chain Hydrocarbons in Electrical Discharges: Absorption and Fluorescence Study of $C_{11}H_9^+$ and $C_{11}H_9^\bullet$ Isomers in Neon Matrices

Adam Nagy, Jan Fulara,† and John P. Maier*

Department of Chemistry, University of Basel, Klingelbergstrasse 80, CH-4056 Basel, Switzerland

Supporting Information

ABSTRACT: A set of arenes (phenylacetylene, indene, and naphthalene cations and $C_{11}H_9^+$ isomers) was produced from 2,4-hexadiyne diluted in helium in a hot-cathode discharge source. The mass-selected ions were codeposited with neon at 6 K and investigated by electronic absorption spectroscopy. This reveals that fused-ring species are readily formed from an acyclic precursor in such a source. After photobleaching of matrices containing $C_{11}H_9^+$, neutral $C_{11}H_9^\bullet$ radicals were also characterized. Assignment of the observed transitions to different $m/z = 141$ cationic and corresponding neutral isomers is given and supported by experiments using other precursors, fluorescence measurements, and time-dependent density functional and second-order approximate coupled cluster calculations.

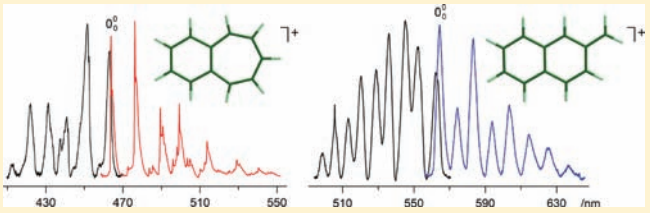

1. INTRODUCTION

Aromaticity not only is a core concept in organic chemistry but also is of astrophysical interest. For instance, polycyclic aromatic hydrocarbons (PAHs) and their derivatives have raised attention since they were proposed as carriers of diffuse interstellar[1] as well as unidentified infrared bands.[2] They are also assumed to play an important role in young Earth-like planetary atmospheres such as that of Titan.[3]

It is generally agreed that the initial step in the growth of PAHs is the ring closure of two propargyl units to benzene.[4−6] Two mechanisms have been put forward for the formation of larger species. The first involves stepwise hydrogen abstraction from the reacting hydrocarbon followed by acetylene addition (HACA);[7−9] the other considers resonance-stabilized free radicals to be the key compounds toward PAHs.[10−13] Both these routes originate from combustion or premixed flame studies, where PAHs are believed to be intermediates in soot formation.[14,15] Although the interstellar medium lacks the two single most important characteristics of the latter environments, high pressure and temperature, the long time scales may compensate for the lower reaction rates in cold, vacuum conditions.

In order to identify such species unambiguously, rather than restrict oneself to mass spectrometric investigations and chemical models, spectroscopic studies on PAH derivatives are desirable. However, these are often hindered by the unavailability of suitable precursors and alternative "synthesis" methods need to be employed. Among others,[16−18] diagnosis of open-chain and cyclic molecules in discharges have suggested the production of PAH-related compounds.[19,20] In this contribution, a series of (fused-)ring hydrocarbon cations was produced from acyclic precursors and trapped in 6 K neon matrices. The reported electronic absorption and fluorescence spectra of $C_{11}H_9^+$ and $C_{11}H_9^\bullet$ may support a better understanding of intermediate steps of PAH formation.

2. METHODOLOGY

The setup employed has been described.[21] Cations of interest were produced in a hot-cathode discharge source from precursor mixtures with helium. The source is similar to conventional electron impact except that the electrons emitted from a hot (∼2000 °C) tungsten filament are confined to a central region by a voltage of ∼50 V applied on a cylindrical anode, and an electromagnetic coil. Chemistry occurs in the resulting plasma, where ionization, fragmentation, and ion−molecule reactions take place.

After extraction from the source, ions were guided using a series of electrostatic lenses through a 90° static deflector, where they were separated from neutrals, to a quadrupole mass filter. Cations mass selected at approximately ±0.5 u resolution were codeposited with a mixture of neon and an electron scavenger (chloromethane)[21,22] for a few hours onto a rhodium-coated sapphire substrate kept at 6 K to build a matrix of ∼150 μm in thickness.

The detection system consists of a halogen or a high-pressure xenon light source, a spectrograph equipped with three gratings blazed at different wavelengths, and two range-specific CCD cameras. Absorption spectra were recorded in the 250−1100 nm region by propagating broadband light through the matrix parallel to its surface in a "waveguide" manner. The effective path length was about 20 mm. Light exiting the sample was collected and transferred with a bundle of 50 optical fibers to the spectrograph. Cut-off filters were used during recording of the spectra to eliminate possible photoconversion of the trapped species by the broadband light. Furthermore, scans were started from the near-IR and continued into the UV; the procedure was later repeated to test

Received: July 13, 2011
Published: October 17, 2011

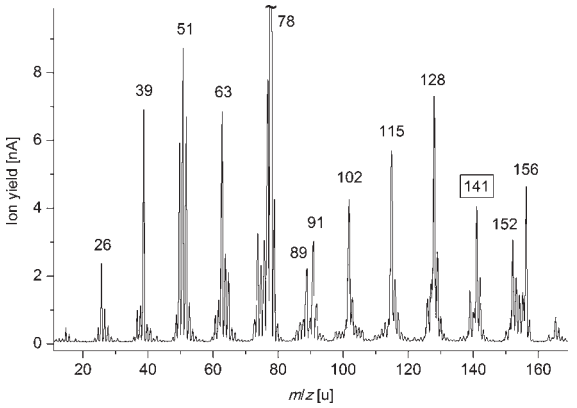

Figure 1. Mass spectrum produced from 2,4-hexadiyne in a hot-cathode discharge ion source.

whether the species were light-sensitive. Subsequently, the matrix was irradiated for 30−60 min with water-filtered radiation of a medium-pressure mercury (mpHg) lamp to neutralize the trapped cations ("photobleaching"), and spectra were recorded anew.

Wavelength-dispersed fluorescence spectra were obtained by exciting the species embedded in neon at an angle of incidence ~45° with a pulsed, Nd^{3+}:YAG-pumped, tunable optical parametric oscillator laser with bandwidth 3−8 cm^{-1} and energies 2−30 mJ. The emission data were collected perpendicular to the matrix surface−the light was focused with a short-focus lens into the optical fiber bundle and transmitted to the same spectrograph and cameras as were used for the absorption measurements. Fluorescence spectra were recorded in 50−60 nm overlapping sections by exciting each distinct absorption band seen obtained after depositing $C_{11}H_9^+$ cations. The signal was accumulated over ~1000 laser shots per section. The excitations were started from the longest-wavelength absorptions and continued to the UV. The fluorescence was measured starting 2 nm from the excitation wavelength upward to avoid saturation of the CCDs with scattered laser light and continued to ~650 nm.

Ground-state harmonic frequencies and excitation energies were computed at different levels of theory using the Gaussian 03 or Turbomole program suites.[23,24]

3. EXPERIMENTAL OBSERVATIONS

Mass spectra of a number of hydrocarbons were recorded to search for precursors for the synthesis of unsaturated carbon chains. Under certain experimental conditions, besides the parent and fragment cations, a growth in the size of ions was observed. For example, in the mass spectrum of 2,4-hexadiyne (2,4-HDy), several prominent peaks corresponding to heavier species than the parent $C_6H_6^+$ (m/z = 78) are present (Figure 1). They form a series in which neighboring members differ notably by 24 or 26 mass units. These are at 102, 128, 152, and 156 u and correspond to $C_8H_6^+$, $C_{10}H_8^+$, $C_{12}H_8^+$, and $C_{12}H_{12}^+$, respectively. Because the parent of 2,4-HDy is isoelectronic with the benzene cation, the question as to the structure of these ions produced from the acyclic precursor arises. The m/z = 102 and 128 species generated from 2,4-HDy were selectively deposited into neon matrices and their absorptions recorded. In the case of $C_8H_6^+$, the spectrum obtained contains phenylacetylene$^+$,[25−27] whereas the trapping of $C_{10}H_8^+$ resulted in bands of naphthalene cation, known from previous matrix isolation and gas-phase studies[27−30] (Figure S1, Supporting Information). These experiments show that small-sized PAH$^+$s are produced from an open-chain precursor in ion−molecule reactions that take place in the discharge-type source. This is consistent with the HACA sequence of PAH growth.[4−6]

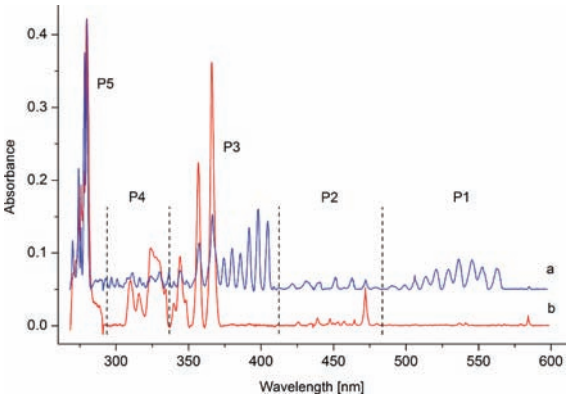

Figure 2. Overview plots of electronic absorption spectra recorded after deposition of $C_{11}H_9^+$ cations (m/z = 141) produced from 1-methyl-naphthalene as precursor into a neon matrix (a) containing CH_3Cl and (b) without an electron scavenger. Regions P1−P3 and P5 are shown in detail in Figures 3−6.

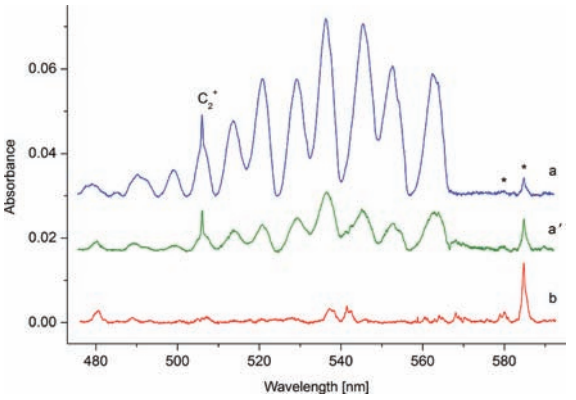

Figure 3. P1 part of the electronic absorption spectrum of $C_{11}H_9^+$ produced from 1-methyl-naphthalene recorded after (a) deposition into neon and (a′) irradiating the matrix with a medium-pressure mercury lamp. Trace b was obtained from the same precursor in an experiment without an electron scavenger. Weak neutral $C_{11}H_9^\bullet$ bands in trace a are marked with asterisks. C_2^+ is a common impurity.

However, in the mass spectrum of 2,4-HDy (Figure 1) between the bands corresponding to PAH$^+$s with an even number of carbon atoms, there are peaks differing from these by 12−14 u. They are at 89, 91, 115, and 141 u and belong to $C_7H_5^+$, $C_7H_7^+$, $C_9H_7^+$, and $C_{11}H_9^+$, respectively. Their presence indicates that the growth of PAHs proceeds by incorporation of CH_x (x = 0−2) groups into smaller intermediates. Apart from minor intensity gain of a few peaks (e.g., those at 26 and 116 u), the mass spectrum remains identical to Figure 1 after mixing acetylene to the 2,4-HDy precursor.

$C_7H_7^+$ was studied recently in 6 K neon matrices and two isomers were detected: tropylium and benzylium.[31] $C_9H_n^+$ (n = 7−9) species are the topic of ongoing investigations.[32] In this contribution, the structure of the $C_{11}H_9^+$ cations is the focus.

3.1. Absorption Measurements. Several electronic band systems have been detected in the 250−600 nm range following the deposition of m/z = 141 cations produced from 1-methyl-naphthalene (1-MetN) into a neon matrix containing a small

admixture of chloromethane (Figure 2a). Normally, during the trapping of cations, corresponding neutrals are also formed in the matrix via recombination of the ions with free electrons ejected from metal surfaces.[21,22] To distinguish absorptions of cations from those of neutrals, $C_{11}H_9^+$ generated from the same precursor was deposited also into a "pure" neon matrix. The spectrum obtained is Figure 2b; it corresponds to neutral $C_{11}H_9^\bullet$, because the neutralization of cations is highly efficient in cases when no electron scavenger is used.[21,22] The spectra of $C_{11}H_9^+$ and its neutral radical are quite complex and likely originate from more than one species. Five distinct regions (P1−P5) can be recognized (Figure 2).

The P1 part is in Figure 3 and shows the absorptions measured after deposition of $C_{11}H_9^+$ produced from 1-MetN (upper trace), the change of the spectrum upon UV irradiation of the matrix with a mpHg lamp (middle), and the bands of neutral $C_{11}H_9^\bullet$ recorded for the same precursor in a "pure" neon matrix (bottom). The peak labeled C_2^+ is a minor fragmentation product of some of the mass-selected ions which arrive with high kinetic energy at the substrate surface.[33] UV photons bleach the absorptions with onset at 562.2 nm indicating the cationic nature of the system. These bands were also observed using several different precursors or precursor mixtures for the generation of $C_{11}H_9^+$ cations, e.g., 2-methyl-naphthalene (2-MetN), 1-phenyl-4-penten-1-yne (PPey), phenylacetylene + propyne, benzyl chloride + diacetylene, or 2,4-HDy + acetylene. The relative band intensity of the 562 nm system remained the same in all experiments illustrating a common origin. It has an extended vibrational progression, which is built on five normal modes of energy 326, 528, 866, 1120, and 1429 cm^{-1} and their combinations. Wavelengths of the cationic absorption band maxima are collected in Table 1.

Table 1. Observed Absorption Band Maxima ($\lambda_{Ne} \pm 0.1$ nm) of Electronic Transitions of $C_{11}H_9^+$ Cationic Isomers in 6 K Neon Matrices and Assignments

λ_{Ne} (nm)	ν (cm^{-1})	$\Delta\nu$ (cm^{-1})	assignment[a]
		2-Naphthylmethylium (2-NyMe$^+$)	
562.2[b]	17 787	0	0_0^0 $1^1A' \leftarrow X^1A'$
552.1	18 113	326	ν_{37}
546.0	18 315	528	ν_{34} [or ν_{33}]
536.1	18 653	866	ν_{30} [or ν_{37} + 528]
528.9	18 907	1120	ν_{26} [or 2 × 528]
520.4	19 216	1429	ν_{16} [or 2 × 528 + ν_{37}]
513.4	19 478	1691	[3 × 528]
505.7	19 775	1988	$\nu_{26} + \nu_{30}$ [or 3 × 528 + ν_{37}]
498.7	20 052	2265	
490.7	20 379	2592	
404.5	24 722	0	0_0^0 $2^1A' \leftarrow X^1A'$
398.0	25 126	404	ν_{36}
391.7	25 530	808	$2\nu_{36}$
385.5	25 940	1218	$3\nu_{36}$
379.9	26 323	1601	$4\nu_{36}$
374.2	26 724	2002	$5\nu_{36}$
369.1	27 093	2371	$6\nu_{36}$
363.5	27 510	2788	$7\nu_{36}$
		Benzotropylium (BzTr$^+$)	
462.6[b]	21 617	0	0_0^0 $1^1B_1 \leftarrow X^1A_1$
451.1	22 168	551	ν_{18}
440.1	22 722	1105	$2\nu_{18}$
430.9	23 207	1590	$3\nu_{18}$ [or ν_6]
421.8	23 708	2091	$4\nu_{18}$ [or ν_{18} + 1590]
336.3	29 735	0	0_0^0 $1^1A_1 \leftarrow X^1A_1$
329.9	30 312	577	ν_{18}
325.9	30 684	949	ν_{15}
321.8	31 075	1340	ν_{10}
278.4	35 920	0	0_0^0 $2^1A_1 \leftarrow X^1A_1$
274.2	36 470	550	ν_{18}
267.4	37 397	1477	ν_8
457.5	21 858	0	isomer C$^+$
436.9	22 889	0	isomer A$^+$
430.5	23 229	340	
421.3	23 736	847	
417.5	23 952	1063	
412.0	24 272	1383	
404.5	24 722	1833	
391.7	25 530	0	isomer B$^+$

[a] Vibrational assignment in the excited states is based on totally symmetric modes (cm^{-1}) in the ground state of 2-NyMe$^+$ (a′ in C_s), 3170, 3135, 3128, 3123, 3114, 3112, 3110, 3105, 3077, 1604, 1583, 1547, 1513, 1485, 1453, 1439, 1399, 1369, 1360, 1334, 1277, 1237, 1196, 1175, 1157, 1126, 1012, 987, 930, 882, 740, 712, 614, 505, 452, 406, and 275, and BzTr$^+$ (a_1 in C_{2v}), 3134, 3117, 3111, 3093, 3083, 1570, 1504, 1488, 1468, 1378, 1250, 1192, 1179, 1034, 946, 889, 688, 563, and 406, calculated with DFT at the BLYP/cc-pVTZ level of theory (unscaled), as well as on fluorescence measurements (in square brackets, see section 3.2). See the Supporting Information for the frequencies of 1-NyMe$^+$. [b] Based on the combined absorption and fluorescence (section 3.2) data, the zero-phonon lines of the onsets of the referred electronic transitions are at 563.2 (2-NyMe$^+$) and 463.8 nm (BzTr$^+$). [c] These features were observed only when chain or ring−chain precursors were used for the production of $C_{11}H_9^+$. Assignment of the transitions to different isomers is given in section 4.1.

In the top trace of Figure 3, absorptions of neutral $C_{11}H_9^\bullet$ are also seen; these are the band at 584.2 nm and a very weak one at 579.6 nm. They grow in intensity upon UV irradiation of the matrix (middle trace) and are better discernible when no electron scavenger was used for the trapping of cations (bottom). In the latter spectrum, there are more neutral bands; they lie 136, 504, 632, 740, 1371, and 1512 cm^{-1} above the origin at 584.2 nm. Wavelengths of the observed $C_{11}H_9^\bullet$ absorptions are listed in Table 2.

In the past, $C_{11}H_9^\bullet$ radicals produced by the UV photolysis of 1- or 2-MetN in frozen *n*-paraffin glassy solutions were studied by luminescence methods—wavelength-dispersed phosphorescence and fluorescence spectra of 1- and 2-naphthylmethyl (1- and 2-NyMe$^\bullet$) have been reported.[34] The origin band of transitions of the former and latter species in *n*-hexane lies at 588 and 598 nm, respectively, spaced ∼290 cm^{-1} from one another. Several vibrational frequencies have also been derived from their structured emission; they are, among others, 519, 1389, and 1598 cm^{-1} for 2-NyMe$^\bullet$, which are close to observed ones for $C_{11}H_9^\bullet$ embedded in neon (Table 2), though the former refer to

Table 2. Absorption Band Maxima ($\lambda_{Ne} \pm 0.1$ nm) of Electronic Transitions of $C_{11}H_9^{\bullet}$ Neutral Radicals in 6 K Neon Matrices and Assignments

λ_{Ne} (nm)	ν (cm^{-1})	$\Delta\nu$ (cm^{-1})	assignment[a]	
		2-Naphthylmethyl (2-NyMe$^{\bullet}$)		
584.2	17 117	0	0_0^0	$1^2A' \leftarrow X^2A''$
579.6	17 253	136	ν_{37}	
567.5	17 621	504	ν_{34}	
563.4	17 749	632	ν_{33}	
560.0	17 857	740	ν_{31}	
540.9	18 488	1371	ν_{17}	
536.8	18 629	1512	ν_{12}	
506.5	19 743	2626		
488.4	20 475	3358		
479.9	20 838	3721		
472.2	21 177	0	0_0^0	$2^2A' \leftarrow X^2A''$
464.5	21 529	352	ν_{36}	
457.4	21 863	686	ν_{32}	
453.5	22 051	874	ν_{30}	
447.6	22 341	1164	ν_{23}	
438.9	22 784	1607		
366.4	27 293	0	0_0^0	$6^2A' \leftarrow X^2A''$
357.0	28 011	718	ν_{32}	
348.4	28 703	1410	$2\nu_{32}$	
344.4	29 036	1743		
340.0	29 412	2119	$3\nu_{32}$	
334.6	29 886	2593		
330.7	30 239	2946		
323.8	30 883	3590		
315.9	31 656	4363		
310.2	32 237	4944		
		1-Naphthylmethyl (1-NyMe$^{\bullet}$)		
579.6	17 253	0	0_0^0	$1^2A' \leftarrow X^2A''$
357.0	28 011	0	0_0^0	$3^2A' \leftarrow X^2A''$
		Ring−Chain Neutrals[b]		
485.5	20 597	0	isomer A$^{\bullet}$	
464.5	21 529	0	isomer B$^{\bullet}$	
447.6	22 341	0	isomer C$^{\bullet}$	
		Benzocycloheptadienyl (BzCh$^{\bullet}$)		
280.2	35 689	0	0_0^0	$4^2A_1 \leftarrow X^2B_1$
277.8	35 997	308	ν_{19}	
275.9	36 245	556	ν_{18}	
274.2	36 470	781	ν_{16} or ν_{17}	
272.2	36 738	1049	ν_{14}	

[a] See the Supporting Information for ground-state harmonic frequencies. [b] These features were detected only when chain or ring−chain starting materials were used for the production of $C_{11}H_9^+$, followed by neutralization. Assignment of the observed transitions to different isomers is given in section 4.2.

the ground state of the radical. This suggests that the neutral system with onset at 584.2 nm in a neon matrix originates from 2-NyMe$^{\bullet}$ and the weak band 136 cm^{-1} below (at 579.6 nm) belongs to 1-NyMe$^{\bullet}$.

This assignment is corroborated by a recent resonance-enhanced multiphoton ionization study on the 1- and 2-NyMe$^{\bullet}$ radicals generated from 1- or 2-MetN.[35] Both isomers of NyMe$^{\bullet}$ have been formed from each precursor. The onset of the electronic transition of 2-NyMe$^{\bullet}$ (at 583.6 nm) lies close to the origin band of $C_{11}H_9^{\bullet}$ at 584.2 nm in a neon matrix. The onset of 1-NyMe$^{\bullet}$ in the gas phase is located at somewhat shorter wavelength, 106 cm^{-1} from that of 2-NyMe$^{\bullet}$. This value is close to the one extracted from the neon matrix spectrum (136 cm^{-1}) for the weak band next to the origin at 584.2 nm. The spacing of 290 cm^{-1} obtained from the separation of the emissions of the two NyMe$^{\bullet}$ isomers in frozen *n*-hexane[34] is larger due to a more perturbative environment.

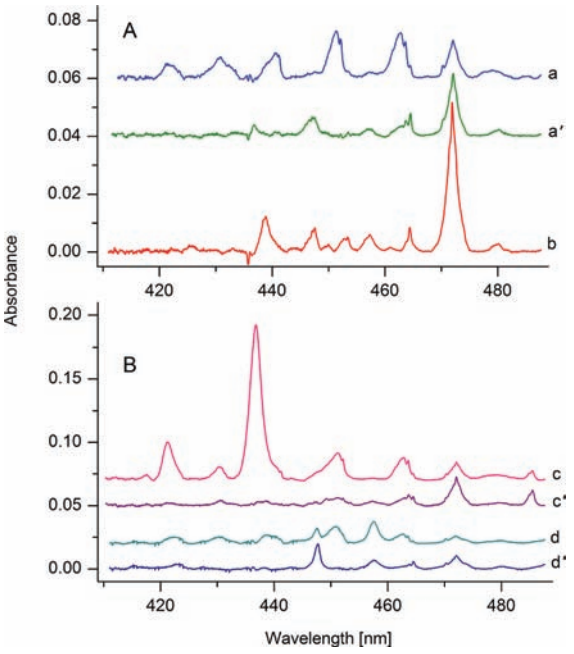

Figure 4. P2 part of the electronic absorption spectrum of $C_{11}H_9^+$. (A) The cations were produced from 1-methyl-naphthalene and the spectra recorded after (a) deposition and (a′) irradiation; trace b was obtained from the same precursor without an electron scavenger. (B) $C_{11}H_9^+$ was generated from 1-phenyl-4-penten-1-yne or a 2,4-hexadiyne + acetylene mixture, and the spectra were measured after (c, d) deposition and (c′, d′) subsequent UV bleaching, respectively.

To summarize, neutralization of $C_{11}H_9^+$ produced from 1-MetN leads to the formation of both 1- and 2-NyMe$^{\bullet}$ radicals in the matrix; absorptions of the latter are stronger than that of the former. This reflects a higher concentration of 2-NyMe$^{\bullet}$ than 1-NyMe$^{\bullet}$ in the neon matrices of the present study or a larger oscillator strength of its transition or both. It can also be concluded that both naphthylmethylium cations (1- and 2-NyMe$^+$) should be present trapped in the matrix in these experiments and that 1-NyMe$^+$ formed from 1-MetN isomerizes in the ion source, because a 1-/2-NyMe$^{\bullet}$ rearrangement in the rigid matrix as alternative is hindered.

In the P2 range, weak absorptions have been detected following the deposition of $C_{11}H_9^+$ produced from 1-MetN (Figure 4A, upper trace). The same bands were observed in spectra obtained for all other precursors used for the generation of the cations, including 2,4-HDy. That at 462.6 nm and four accompanying ones at shorter wavelengths decay after UV irradiation of the matrix (Figure 4A, middle trace). Their similar shape (a broad feature and a sharp, long-wavelength shoulder) and identical behavior upon photobleaching indicate that they belong to a system of one

dx.doi.org/10.1021/ja206522s |*J. Am. Chem. Soc.* 2011, 133, 19796–19806

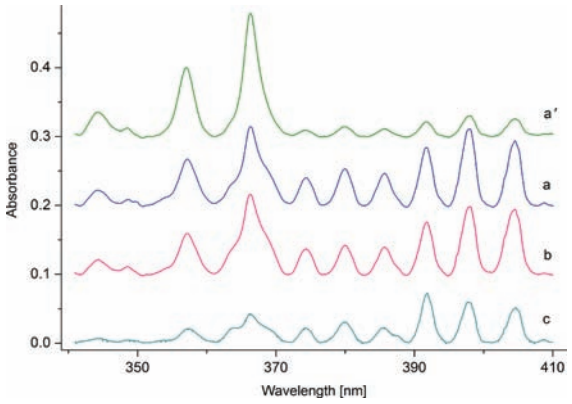

Figure 5. P3 part of the electronic absorption spectrum of $C_{11}H_9^+$ produced from (a) 1-methyl-naphthalene, (b) 1-phenyl-4-penten-1-yne, and (c) 2,4-hexadiyne + acetylene. Trace a′ was measured after irradiating the matrix corresponding to trace a.

isomer of $C_{11}H_9^+$. The spectrum looks simple; the 462.6 nm band is the onset and those at higher energies are the fundamental and overtone vibrations of 551 cm^{-1}. The relative intensity of this 463 nm system and the 562 nm one (Figure 3) varied in spectra obtained under different discharge conditions in the source and with the precursors used; hence, they belong to two $C_{11}H_9^+$ isomers.

Apart from the cationic absorptions, neutral ones are also present in trace a of Figure 4A. Their intensity increases at the expense of the photoneutralized $C_{11}H_9^+$ cations (trace a′). The most prominent (origin) band of neutral $C_{11}H_9^•$ was detected at 472.2 nm in this part of the spectrum. It is also present, together with weaker absorptions at shorter wavelengths, in the spectra obtained for every starting material studied and is better seen in trace b, measured in a neon matrix without CH_3Cl. The band at 464.5 nm forms another system, because its ratio to that at 472.2 nm varied in different experiments. However, the 472.2 nm peak and that at 584.2 nm of 2-NyMe$^•$ (Figure 3b) preserved a constant intensity rate in every recording.

Besides the cationic and neutral systems discussed above, new absorptions, unique to some of the precursors used, have been detected in the P2 spectral range (Figure 4B). When the $C_{11}H_9^+$ cations were generated from PPey and embedded into a neon matrix, a strong cationic system with onset at 436.9 nm (trace c) appeared that decayed upon UV irradiation. Simultaneously, a neutral absorption at 485.5 nm grew (trace c′). These two features were also seen, although weaker, in experiments using 1,6-heptadiyne + diacetylene, phenylacetylene + propyne, or benzyl chloride + diacetylene mixtures for ion production. The conclusion is that the plausible structure of this $C_{11}H_9^+$ isomer and its respective radical is a benzene ring fused with an aliphatic chain.

Other new absorptions have also been detected, characteristic for the 2,4-HDy + acetylene mix as the precursor of $C_{11}H_9^+$ (Figure 4B). The onset of a cationic system lies at 457.5 nm (trace d) and that of a neutral one at 447.6 nm (trace d′). These $C_{11}H_9^•$ and $C_{11}H_9^+$ isomers likely have similar "head-and-tail" structure to the pair above (a chain attached to benzene), because their bands lie in the same spectral region.

In the 340−410 nm range (P3 part of the spectrum), strong, structured absorptions have been detected following the deposition of $C_{11}H_9^+$ produced from 1-MetN into neon (Figure 5, trace a). The system with origin at 404.5 nm has a long, regular progression built on the 404 cm^{-1} mode and decreases in intensity upon irradiation of the matrix with UV photons (trace a′). Concurrently, another system with onset at 366.4 nm becomes stronger. The 366.4 nm band has two broad, long- and short-wavelength shoulders, which belong to the 404 nm cationic system, because they behave in a similar way upon irradiation. The band at 357.0 nm gains intensity upon exposure to UV photons, however, not as much as that at 366.4 nm does. The reason could be a wavelength coincidence of the former absorption with another cationic system or it may be the onset of an electronic transition of another isomer of neutral $C_{11}H_9^•$. Both the 404 cationic and 366 nm neutral systems were present in the spectra obtained for all precursors used for generation of the ions. The former maintained a constant intensity ratio with the 562 nm system, whereas the strength of the bands starting at 366.4 nm of neutral $C_{11}H_9^•$ correlated well with the absorption of 2-NyMe$^•$ at 584.2 nm and the 472 nm system.

Because of this coherence and that in earlier studies fluorescence of 2-NyMe$^•$ in frozen *n*-hexane was observed when the 2-MetN sample was excited with the 365 nm mercury line,[34] the 366 nm system is assigned to the 2-NyMe$^•$ radical. From that study, it can also be expected that 1-NyMe$^•$ has a transition in the same region, because its emission was observed upon excitation with the same mercury line. The best candidate for this transition in solid neon is the 357.0 nm band, whose intensity changes in a different manner to that at 366.4 nm. In glassy matrices, bands are broader and shifted in comparison to solid neon; therefore, it was possible to excite both isomers of NyMe$^•$ using the same mercury line. At ∼357 nm lies also the first vibrational band of the 366 nm system of 2-NyMe$^•$ (718 cm^{-1} to the blue of the origin), because its first overtone at 1410 cm^{-1} can be well discerned in the neon matrix spectrum. The onset of the transition of 1-NyMe$^•$ is likely hidden underneath this band.

The relative intensity of the first three absorption bands of the 404 nm system varies with the precursor used. In most experiments, the intensity pattern was as Figure 5, trace a, shows for 1-MetN: the second band is the strongest. However, in the case of PPey, the first and second have similar strength (trace b), because a vibrational band of the 437 nm system (Figure 4B, trace c) overlaps with the origin of the 404 nm transition. In the case of 2,4-HDy + acetylene, the third band at 391.7 nm is the strongest in this part of the spectrum (Figure 5c); this could be the onset of the second transition of the $C_{11}H_9^+$ isomer for which the first system is observed at 457.5 nm (Figure 4B, trace d) or it is due to another isomer of $C_{11}H_9^+$.

The P4 part of the spectra of $C_{11}H_9^+$ (Figure 2, 290−340 nm range) has a number of weak, cationic absorptions as well as some of neutral origin. Due to their low intensity and complexity, it is difficult to associate them with any of the systems discussed above.

The strongest absorptions have been detected in the P5 UV range after deposition of $C_{11}H_9^+$ produced from 1-MetN (Figure 6, blue trace). Two systems can be seen: a cationic with onset at 278.4 nm and one associated with neutral $C_{11}H_9^•$ commencing at 280.2 nm. The former loses intensity, while the latter becomes stronger upon UV irradiation (green trace). The 278 nm system of $C_{11}H_9^+$ is more discernible in an experiment using a phenylacetylene + propyne precursor mixture (magenta); three vibrational bands are apparent. An accurate measure of band intensities is problematic in the UV because of the strong light scattering in neon matrices—the optical path (and, thus, the absorbance) changes with the wavelength of the probing light. Additionally, in most experiments carried out in this study, the

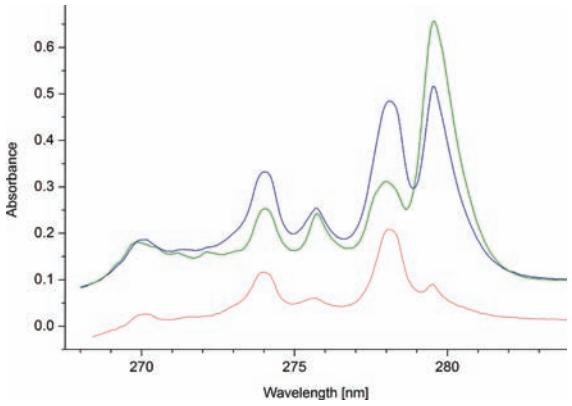

Figure 6. P5 part of the electronic absorption spectrum of $C_{11}H_9^+$ produced from 1-methyl-naphthalene after deposition (blue trace) and after photobleaching the matrix (green). Cationic bands are better discernible in the spectrum from another experiment using a phenyl-acetylene + propyne precursor mixture (magenta).

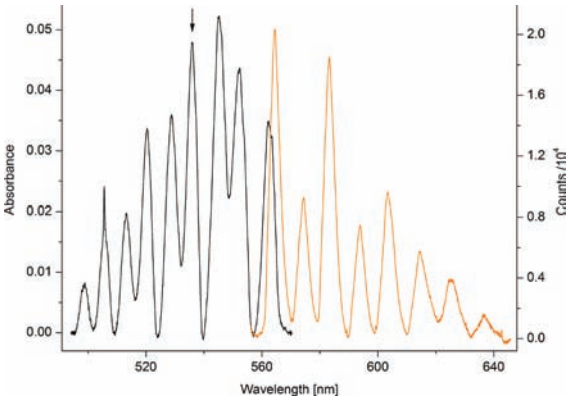

Figure 7. Electronic absorption (left) and fluorescence (right) spectra of $C_{11}H_9^+$ recorded after depositing the cations produced from 1-phenyl-4-penten-1-yne into a neon matrix. The emission trace was obtained upon exciting the 536.8 nm feature (arrow) of the 562 nm absorption system. The intersection of the two spectra shows that the zero-phonon line of the origin bands is at 563.2 nm.

absorptions in this region were saturated due to the high oscillator strength of transitions of the trapped species. Moreover, the bands of $C_{11}H_9^+$ and $C_{11}H_9^\bullet$ overlap. All these effects preclude a rational comparison of their intensity with the systems discussed previously.

3.2. Fluorescence Spectra. All the prominent bands in the absorption spectrum recorded after depositing $m/z = 141$ cations produced from PPey into neon have been excited with a pulsed, tunable laser in order to obtain wavelength-dispersed emission of the trapped species. PPey was chosen as the precursor of $C_{11}H_9^+$ for the fluorescence studies because it shows all the systems that were observed using 1-MetN (Figure 2a); additionally, the 437 nm system, specific for chain and ring−chain precursors, is also present (Figure 4B, trace c). The search for emission features was started by exciting the longest-wavelength prominent absorption band at 562.2 nm (Figure 3) and continued toward the UV.

The excitation at 562.2 nm resulted in a structured emission starting at ~574 nm. The (origin) band at around 562 nm could not be observed in this case, because measurements were started at a wavelength 2 nm longer than the excitation one in order to avoid overexposure of the CCD from the strong laser scatter. Upon exciting the next absorption band of the 562 nm system, an emission at 564.8 nm, together with the features seen before, appeared. The spectrum obtained for the excitation wavelength 536.8 nm, along with the 562 nm absorption system, is shown in Figure 7. The two are similar; the fluorescence corresponds to the 562 nm system of $C_{11}H_9^+$. Origins of the emission and absorption spectra overlap in the region where the bands have weak short- or long-wavelength shoulders, respectively, at 563.2 nm. This is the zero-phonon line (ZPL) of the onsets of the two spectra.

The 565 nm fluorescence system of $C_{11}H_9^+$ has a regular pattern: strong and weak bands alternate. The former is based on the fundamental and overtone vibrations of the mode 573 cm^{-1}, which is active in the ground state of $C_{11}H_9^+$. The weaker ones are associated with the 311 cm^{-1} vibration (first band) and its combinations with the 573 cm^{-1} fundamental (the remaining ones). In absorption, the first two bands correspond to modes of 326 and 528 cm^{-1}, respectively. However, this latter system of $C_{11}H_9^+$ is more complicated than the fluorescence. The third band lies 866 cm^{-1} above the origin; it is 14 cm^{-1} higher in energy than the combination of the two modes above. The fourth absorption corresponds to a 1120 cm^{-1} vibration, which exceeds the overtone value of the 528 cm^{-1} mode by 64 cm^{-1}. Likely, more fundamentals are active in the 562 nm absorption system than in the corresponding fluorescence one (Tables 1 and 3), but not all are well-resolved, for example, between every second band of the former spectrum the absorbance does not reach the baseline. The absorption measurements showed that the intensity of the 562 nm system correlates well with that of starting at 404.5 nm; however, no emission has been detected upon excitation of individual bands of the latter system.

Another strong emission with onset at ~464 nm has been detected when the laser was scanned across the moderately intense absorption system with origin at 462.6 nm. The first three absorption bands of this system have a sharp long-wavelength shoulder (ZPL) imposed onto a broad feature (Figure 8, top left trace). The emission obtained for the excitation of the ZPL of the second absorption band (at 452.1 nm) is shown in the top right trace of the figure. The red trace on the right shows the emission recorded when the maximum of this absorption band (451.1 nm) was excited instead of its ZPL. These two fluorescence spectra have similar appearance and look like mirror images of the 463 nm absorption system. The onset of the first one has a strong, narrow short-wavelength feature preceding a broad one (ZPL and phonon sideband). ZPLs of the origins of the emission and absorption spectra overlap at 463.8 nm. The fluorescence spectrum recorded when the 452.1 nm vibrational band ZPL was excited reveals more detail than that obtained from exciting the maximum of the same band. Many weak, narrow features (ZPLs of the individual vibrations) are resolved in this spectrum; they become smeared out in the second one.

The vibrational energies derived from the ZPL positions of individual fluorescence bands of the 464 nm system (Figure 8, top right) are collected in Table 3. The most prominent emission features originate from relaxation to the two fundamental modes of energy 561 and 1533 cm^{-1} in the ground state of $C_{11}H_9^+$ and their overtones and combinations. The weaker peaks in this spectrum correspond to five other fundamentals: 401, 887, 1182, 1396, and 1485 cm^{-1}, which also form combination bands with the two mentioned above. All the bands (even the weakest ones

Table 3. Fluorescence Band Maxima ($\lambda_{Ne} \pm 0.1$ nm) of Electronic Transitions of $C_{11}H_9^+$ Cationic Isomers in 6 K Neon Matrices and Assignments[a]

λ_{Ne} (nm)	ν (cm^{-1})	$\Delta\nu$ (cm^{-1})	assignment[b]
	2-Naphthylmethylium (2-NyMe$^+$)		
564.8[c]	17 705	0	0_0^0 $X^1A' \leftarrow 1^1A'$
574.9	17 394	311	ν_{37}
583.7	17 132	573	ν_{33}
594.3	16 827	878	$\nu_{33} + \nu_{37}$
603.8	16 562	1143	$2\nu_{33}$
614.8	16 265	1440	$2\nu_{33} + \nu_{37}$
625.8	15 980	1725	$3\nu_{33}$
637.9	15 676	2029	$3\nu_{33} + \nu_{37}$
	Benzotropylium (BzTr$^+$)[d]		
463.8 s	21 561	0	0_0^0 $X^1A_1 \leftarrow 1^1B_1$
472.6	21 160	401	ν_{19}
476.2 s	21 000	561	ν_{18}
483.7	20 674	887	ν_{16}
485.5	20 597	964	$\nu_{18} + \nu_{19}$
489.4 m	20 433	1128	$2\nu_{18}$
490.7	20 379	1182	ν_{12}
495.9	20 165	1396	ν_{10}
498.1	20 076	1485	ν_8
499.3 m	20 028	1533	ν_6
503.5	19 861	1700	$3\nu_{18}$
504.9	19 806	1755	$\nu_{12} + \nu_{18}$
510.3	19 596	1965	$\nu_{10} + \nu_{18}$
512.5	19 512	2049	$\nu_8 + \nu_{18}$
513.7 m	19 467	2094	$\nu_6 + \nu_{18}$
519.6	19 246	2315	$2\nu_{18} + \nu_{12}$
522.4	19 142	2419	$\nu_6 + \nu_{16}$
524.4	19 069	2492	$\nu_6 + \nu_{18} + \nu_{19}$
525.2	19 040	2521	$2\nu_{18} + \nu_{10}$
529.1 w	18 900	2661	$2\nu_{18} + \nu_6$
530.5	18 850	2711	$\nu_6 + \nu_{12}$
536.6	18 636	2925	$\nu_6 + \nu_{10}$
539.3	18 543	3018	$\nu_6 + \nu_8$
540.5 w	18 501	3060	$2\nu_6$
545.5	18 332	3229	$3\nu_{18} + \nu_6$
547.0	18 282	3279	$\nu_6 + \nu_{12} + \nu_{18}$

[a] Fluorescence studies were carried out using 1-phenyl-4-penten-1-yne as precursor for the production of $C_{11}H_9^+$. [b] See footnote a of Table 1 for the totally symmetric vibrational fundamentals. [c] Based on the absorption (section 3.1) and fluorescence measurements, the zero-phonon line of the referred transition is at 563.2 nm. [d] Main spectral features (Figure 8, right) correspond to the two "most active" modes of energy 561 and 1533 cm^{-1} in the ground state of BzTr$^+$; their intensity is indicated as strong, medium, or weak (all others are very weak).

present) can be assigned to specific overtones or combinations of these seven modes. In the case of the 463 nm absorption system, the bands are broader and were recorded at a lower signal-to-noise ratio; as a consequence, only the most prominent bands, corresponding to the excitation based on the two vibrations 551 and 1590 cm^{-1}, have been detected.

The same 464 nm fluorescence system has been seen when weak absorptions in the 290−340 nm range (Figure 8, middle left trace) or the strong one at 278.4 nm (bottom left) were excited. The resulting emission spectra, which belong to the excitation of the 336.3 and 278.4 nm absorption bands of $C_{11}H_9^+$, are shown in green and blue traces, respectively, of the same figure. Their intensity is about 10 and 70 times weaker than that for the excitation of the 463 nm visible absorption system, although the spectra were not normalized for the laser power, which is about an order of magnitude lower in the second harmonic regime, $\lambda < 420$ nm.

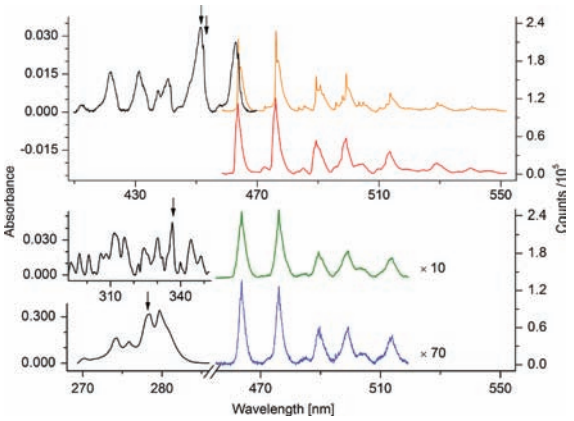

Figure 8. Electronic absorption (left) and fluorescence (right) spectra of $C_{11}H_9^+$ recorded after depositing the cations produced from 1-phenyl-4-penten-1-yne into a neon matrix. Excitation wavelengths of the recorded emission traces are indicated on the corresponding absorption plots by arrows. The orange and red plots were obtained upon exciting the zero-phonon line at 452.1 or the band maximum at 451.1 nm, respectively.

These fluorescence measurements prove that the three absorption systems with onsets at 462.6, ~340, and 278.4 nm belong to the same $C_{11}H_9^+$ isomer. It was not possible to deduce this on the basis of the recorded absorption spectra only, because the intensity of the second system was too modest to reliably relate it to others. Furthermore, the third, strong system with onset at 278.4 nm lies in the UV, where scattering in the matrix has a significant influence on the absorbance measurements; hence, the comparison of its intensity with other ones was also hindered.

The positions of the three correlating absorption systems lie near the wavelengths of broad absorptions of the benzotropylium cation (BzTr$^+$) reported in an acidic solution at 425, 338, and 282 nm.[36] In that study, BzTr$^+$ was produced by dissolving the $LiAlH_4$ reduction product of benzotropone, the pseudobase $C_{11}H_9OH$, in concentrated (60 %) sulfuric acid. Though somewhat different methods were applied for the synthesis of tropylium cation,[37,38] its spectrum in a strong sulfuric acid solution[36,37] agrees well with the one obtained in a 6 K neon matrix following mass-selective ($m/z = 91$) deposition of $C_7H_7^+$ cations.[31] Therefore, the three absorption systems with onsets at 462.6, ~340, and 278.4 nm are assigned to BzTr$^+$.

In summary, the present absorption and emission studies on $C_{11}H_9^+$ and $C_{11}H_9^\bullet$ embedded in neon matrices reveal band systems that originate from several cationic and neutral species. Three absorption systems and the corresponding fluorescence spectrum have been assigned to BzTr$^+$. Absorptions of neutral 1- and 2-NyMe$^\bullet$ have also been identified; their cationic counterparts should also be present in the spectra. There are several systems that remained unassigned; in order to do so, theoretical

Chart 1. Structures of (a) the Four Most Stable and (b) Four Considered Ring−Chain Isomers of $C_{11}H_9^{+a}$

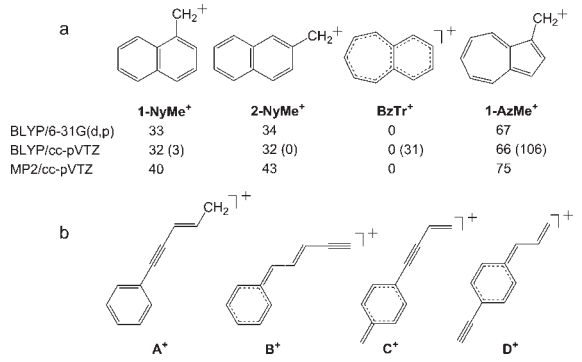

[a]All species are of planar C_s symmetry except $BzTr^+$ (planar C_{2v}). Relative ground-state energies (kJ mol^{-1}, not corrected for zero-point vibrations) of the first four cations as well as the corresponding neutrals (in parentheses) are given at different levels of theory.

calculations on excitation energies of different isomers of $C_{11}H_9^+$ and their neutrals were needed.

4. COMPUTATIONAL RESULTS

4.1. $C_{11}H_9^+$ Cations. The $C_{11}H_9^+$ cations and their corresponding neutrals are relatively large electronic systems (74/75 electrons); hence, they cannot be treated easily with high-level, *ab initio* methods. However, past work from this laboratory has shown that multiple isomers of a mass-selected ion can be trapped in solid neon in copious amounts in two cases: (a) if they partially relax thermally in the ion source and, thus, have energy within ∼50 kJ mol^{-1} of the most stable form or (b) if the product can directly be derived from the precursor by simple chemical reactions. Therefore, in order to select first the lowest-energy isomers of $C_{11}H_9^+$, geometries of expected as well as exotic structures were optimized with density functional theory (DFT) using the BLYP functional[39,40] and a small basis set, 6-31G(d,p). The four most stable structures, $BzTr^+$, 1-$NyMe^+$, 2-$NyMe^+$, and 1-azulenylmethylium (1-$AzMe^+$), are shown together with their relative ground-state energies in Chart 1a. Other possible, higher-energy structures are collected in Chart S1 (Supporting Information).

The geometry of these four fused-ring isomers was then optimized with the same functional and a larger (cc-pVTZ) basis set. The calculations reveal that $BzTr^+$ is the lowest-energy structure on the $C_{11}H_9^+$ potential energy surface. Two closely related species, 1- and 2-$NyMe^+$, have nearly the same energy, lying 32 kJ mol^{-1} above $BzTr^+$. The fourth isomer, 1-$AzMe^+$, is 66 kJ mol^{-1} less stable than $BzTr^+$. The ground-state energies computed using the small basis set agree well with the results obtained with the larger one (Chart 1a); thus, further discussion is restricted to these four most stable isomers.

Vibrational fundamentals were calculated with DFT at the BLYP/cc-pVTZ level of theory for the optimized structures. They can be compared directly with the experimental values derived from the emission spectra of $C_{11}H_9^+$ (Table 3). For instance, in the case of $BzTr^+$, seven modes (401, 561, 887, 1182, 1396, 1485, and 1533 cm^{-1}) have been observed in the fluorescence spectrum (Figure 8, top right). Calculated totally symmetric fundamentals corresponding to the values above are 406, 563, 889, 1179 or 1192, 1378, 1488, and 1504 or 1570 cm^{-1} (Table 1, footnote a). The 1192 and 1570 cm^{-1} theoretical values are better candidates for the experimental 1182 and 1533 cm^{-1} vibrations than the lower-energy ones, because calculations usually overestimate frequencies. The agreement is good and confirms the assignment. The other fluorescence system with onset at 564.8 nm (Figure 7) has a simpler structure based on two vibrations, 306 and 571 cm^{-1}. The latter also forms overtones and combinations with the former one. The calculations predict frequencies 297/567 and 275/614 cm^{-1} for 1- and 2-$NyMe^+$, respectively. Although the former values are closer to the observation, it would be speculative to assign the 565 nm system to 1-$NyMe^+$ based on such small number of vibrations. The calculated frequencies can also be used as a guide for the assignment of vibrational bands of the electronic absorption systems observed in a neon matrix; however, a worse agreement is expected because the latter correspond to the excited state (Table 1).

Knowledge of the electronic energy levels and transition moments of a specific ion is crucial for the assignment of observed electronic systems to that species. Therefore, vertical excitation energies of the four aromatic isomers discussed above (Chart 1a) were calculated using time-dependent (TD) DFT method[41] with the same BLYP functional and cc-pVTZ basis set as for their ground state. In addition, the excitation energies were also obtained employing the second-order approximate coupled cluster (CC2) model[42] from ground-state geometries optimized at the second-order Møller−Plesset perturbation theory (MP2) level. The resolution-of-identity approximation was used also, which replaces four-center, two-electron integrals by three-center ones.[43] The excitation energies of $BzTr^+$ and 1- and 2-$NyMe^+$ computed using these two methods are collected along with their oscillator strengths in Table 4 and compared with the experimental values. A rough correlation can be seen; however, discrepancies are not exceptional even for quite small molecules using state-of-the-art theoretical approaches.[44,45] Although the TD DFT results show a somewhat better match with the observed transition energies, the higher-level CC2 data were considered for comparison; these are shown as stick diagrams together with the absorption spectrum of $C_{11}H_9^+$ in Figure 9. The results for 1-$AzMe^+$ are listed in Table S1 (Supporting Information).

The theoretical excitation energies of $BzTr^+$ can be used to test their reliability, because the electronic systems of this cation have already been assigned on the basis of experiments only. The strongest transition has an energy 4.91 eV (around 253 nm, oscillator strength $f = 0.91$) calculated by CC2; it is overestimated by 0.46 eV with respect to that detected at 278.4 nm. If a similar shift is applied to the two other, low-energy transitions calculated, then the origins of these weak systems are expected at around 471 and 361 nm. These are close to those observed at 463.8 and ∼340 nm. In the latter case, the origin likely lies at somewhat lower wavelength and is masked by other absorptions.

Of the two $NyMe^+$ cations, the stick diagram of 2-$NyMe^+$ (Figure 9, trace b) resembles more the remaining two "main" band systems of $C_{11}H_9^+$. The predicted intense transition of 2-$NyMe^+$ at 3.66 eV (339 nm, $f = 0.37$) needs to be shifted by −0.59 eV to match the observed strong origin band at 404.5 nm. The other, weaker transition of energy 2.24 eV (554 nm) agrees well with the observed system origin at 562.2 nm. Thus, the two systems with onset at 562.2 and 404.5 nm, for which good intensity correlation has been observed in all experiments, are assigned to 2-$NyMe^+$. Because the weak band at 579.6 nm was identified as the origin band of a transition of neutral 1-$NyMe^•$, it

Table 4. Excited-State Symmetries, Vertical Excitation Energies (ΔE) and Transition Oscillator Strengths (f) Computed with Two Methods for the Three Most Stable Isomers of $C_{11}H_9^+$, and Comparison with Experimental Data

	TD DFT//BLYP/cc-pVTZ		CC2//MP2/cc-pVTZ		
excited state	ΔE (eV)	f	ΔE (eV)	f	expt[a] (eV)
		1-NyMe$^+$ (X^1A', planar C_s)			
$1^1A'$	2.21	0.029	2.65	0.12	
$2^1A'$	2.60	0.083	2.90	0.091	
$3^1A'$	4.21	0.052	4.84	0.20	
$4^1A'$	4.43	0.060	5.13	0.0014	
$5^1A'$	4.66	0.0041	5.21	0.029	
$6^1A'$	5.09	0.099	5.71	0.050	
$7^1A'$	5.69	0.14			
$8^1A'$	5.84	0.58			
		2-NyMe$^+$ (X^1A', planar C_s)			
$1^1A'$	1.82	0.027	2.24	0.064	2.21
$2^1A'$	3.35	0.0020	3.66	0.37	3.07
$3^1A'$	3.39	0.18	4.09	0.052	
$4^1A'$	4.67	0.10	5.42	0.064	
$5^1A'$	4.86	0.0077	5.47	0.53	
$6^1A'$	4.93	0.61	5.58	0.39	
$7^1A'$	5.40	0.013			
$8^1A'$	5.67	0.29			
		BzTr$^+$ (X^1A_1, planar C_{2v})			
1^1B_1	2.71	0.014	3.09	0.025	2.68
1^1A_1	3.50	0.0009	3.89	0.0049	3.69
2^1B_1	4.46	0.0051	4.98	0.018	
2^1A_1	4.63	0.64	4.91	0.91	4.45
3^1A_1	5.18	0.021	5.85	0.017	
3^1B_1	5.26	0.21	5.83	0.30	
4^1B_1	5.62	0.044			
4^1A_1	5.76	0.054			

[a] Origin band of electronic transitions of $C_{11}H_9^+$ observed in 6 K neon matrices of this study.

suggests that the 1-NyMe$^+$ cation should also be present. However, its absorptions could not be identified in the experiments; they are probably too weak or hidden underneath strong ones. The energetically least stable cationic isomer of the four in Chart 1a, 1-AzMe$^+$, is unlikely to be present in the neon matrices of this study.

Apart from the absorptions of BzTr$^+$ and 2-NyMe$^+$, three other cationic systems with onset at 457.5, 436.9, and 391.7 nm have been detected. These are precursor-specific: the first and last come together and are only present when a mixture of 2,4-HDy + acetylene was used for generation of the cations; the 437 nm system was the strongest when PPey was used. The structure of $C_{11}H_9^+$ produced mostly from PPey must closely resemble the precursor; namely, constructed from a benzene ring and a hydrocarbon chain (Chart 1b, isomer A$^+$). The other isomer(s) associated with the 2,4-HDy + acetylene mix should have similar, "head-and-tail" structure; three possibilities (B$^+$—D$^+$) are also shown in the same figure.

TD DFT and CC2 calculations were carried out to determine the excitation energies of these four considered ring—chain $C_{11}H_9^+$ isomers. The results are listed in Table S1 (Supporting Information). All isomers have a strong transition in the blue; D$^+$ has two. The CC2 excitation energies and oscillator strengths are as follows: A$^+$ (3.00 eV/413 nm, f = 1.3); B$^+$ (3.23/384, 1.2); C$^+$ (2.94/422, 1.1); and D$^+$ (3.20/387, 0.57; 3.27/379, 0.59). The excitation energy of A$^+$ is not far from the onset of the 437 nm system, and because it has similar structure to the precursor used, PPey, the absorptions are assigned to this cation. The remaining two systems (onsets at 457.5 and 391.7 nm) are tentatively assigned to the C$^+$ and B$^+$ isomers, respectively, because the former has transition at longer wavelength than the latter.

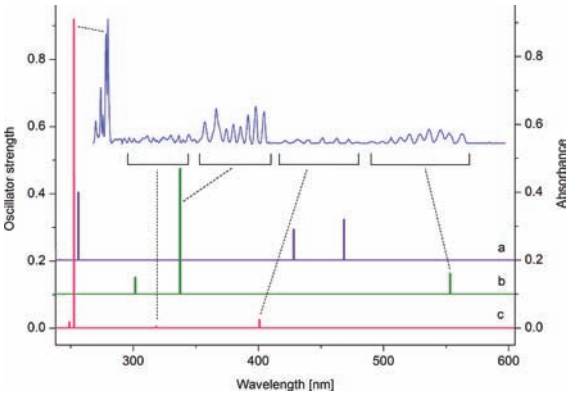

Figure 9. Comparison of the experimentally observed absorptions of $C_{11}H_9^+$ (blue trace) with values calculated at the CC2//MP2/cc-pVTZ level of theory for (a) 1-naphthylmethylium, (b) 2-naphthylmethylium, and (c) benzotropylium.

4.2. $C_{11}H_9^•$ Neutrals. In contrast to $C_{11}H_9^+$ with singlet ground state, the corresponding neutrals are open-shell systems; hence, they are more problematic objects for quantum chemical calculations. Nevertheless, all $C_{11}H_9^•$ isomers of the cations shown in Chart 1 were studied by (TD) DFT and CC2//MP2 methods. As opposed to the cations, the most stable isomer is the 2-NyMe$^•$ radical. Next is 1-NyMe$^•$, predicted 3 kJ mol^{-1} to higher energy, and the benzocycloheptadienyl (BzCh$^•$) radical is at 31 kJ mol^{-1} (Chart 1a). Apart from the ground-state energies, harmonic vibrational frequencies were also calculated with DFT at the BLYP/cc-pVTZ level of theory for the considered $C_{11}H_9^•$ structures. Those of the three "main" bicyclic isomers are collected in footnote a of Table S2 (Supporting Information). These cannot be compared directly with experimental ones, because fluorescence of neutrals has not been detected in this study. However, they were used as a guide for the assignment of the observed electronic absorption spectra of $C_{11}H_9^•$ (Table 2).

The optically allowed electronic transitions from the ground state of $C_{11}H_9^•$ were calculated using TD DFT and CC2 methods, the former with cc-pVTZ and the latter with cc-pVDZ basis set. The excitation energies and oscillator strengths are compiled in Tables S2 and S3 (Supporting Information). Energies of the lowest excited electronic state of 1- and 2-NyMe$^•$ predicted by CC2 are 3.27 and 3.33 eV (379 and 372 nm, f = 0.0009 and 0.0036); they should be compared with the observed ones at 579.6 and 584.2 nm for the former and the latter isomers. The calculations overestimate the energy of these transitions by as much as ~1.2 eV. The agreement between the computed and experimental excitation energies is worse than in the case of $C_{11}H_9^+$. The ~3 times larger value of the so-called *D1* diagnostic[46] for the neutrals than for cations indicates the multireference character of the ground state of the radicals. Therefore, TD DFT calculations are also

expected to describe electronic transitions of neutral $C_{11}H_9^{\bullet}$ worse than those of the cations.

However, TD DFT predicts a weak transition at 2.21 eV (561 nm) with oscillator strength $f = 0.0004$ for 1-NyMe$^{\bullet}$ and at 2.06 eV (602 nm, $f = 0.0015$) for 2-NyMe$^{\bullet}$, which agree well with the observed ones in a neon matrix at 579.6 and 584.2 nm, respectively. A stronger transition ($f = 0.035$) of 2-NyMe$^{\bullet}$ is predicted at 2.63 eV (472 nm), exactly where a medium-intensity neutral system is detected in a neon matrix. The calculated density of states in the experimentally accessible wavelength domain is higher for $C_{11}H_9^{\bullet}$ than in the case of $C_{11}H_9^{+}$. According to the theory, the strongest transitions of 2-NyMe$^{\bullet}$ are located in the UV at 3.76, 4.73, and 4.78 eV (330, 262, and 259 nm) with f values 0.11, 0.29, and 0.14, respectively. The former matches the observed intense system with onset at 366.4 nm, the latter two were not seen in the experiments due to strong scattering in that region. Consequently, the three systems around 584, 472, and 366 nm, which preserved a constant intensity ratio in all recorded spectra, are assigned to the 2-NyMe$^{\bullet}$ radical.

The strongest transitions of 1-NyMe$^{\bullet}$ are predicted around 2.85, 3.17, 4.59, and 4.62 eV (435, 391, 270, and 268 nm) with $f = 0.059$, 0.048, 0.040, and 0.043, respectively. These f values are smaller than the ones calculated for 2-NyMe$^{\bullet}$. Only one weak band at 579.6 nm has been assigned to 1-NyMe$^{\bullet}$. Another candidate is an absorption underneath the first vibrational band of the 366 nm system of 2-NyMe$^{\bullet}$, at 357.0 nm. The weaker oscillator strengths and lower concentration of 1-NyMe$^{\bullet}$ in a neon matrix than for 2-NyMe$^{\bullet}$ are the reasons that no distinct band of this radical could be detected in the spectra.

The most intense neutral absorptions of the overview spectrum, Figure 2b, are in the P5 part (Figure 6). TD DFT foretells the strongest transition of the third "main" neutral isomer, BzCh$^{\bullet}$, at 4.43 eV (280 nm, $f = 0.29$) and several weaker ones around 2.57, 2.81, 3.56, and 4.23 eV (482, 441, 348, and 293 nm) with f values 0.018, 0.0083, 0.0037, and 0.0040, respectively. Exactly at the wavelength predicted for the strong transition of BzCh$^{\bullet}$ is observed the onset of the most intense absorption system of $C_{11}H_9^{\bullet}$ at 280.2 nm in neon; therefore, it is assigned to this radical. Two much weaker transitions predicted around 482 and 441 nm are in the region were the medium-intensity 472 nm system of 2-NyMe$^{\bullet}$ is present and they likely overlap with it. The next calculated weak transition (348 nm) of BzCh$^{\bullet}$ corresponds to absorptions of neutrals present in part P4 of the spectrum recorded without an electron scavenger in the matrix (Figure 2b).

The precursor-dependent bands of $C_{11}H_9^{\bullet}$ neutrals at 485.5, 464.5, and 447.6 nm have already been associated with the cationic transitions at 436.9, 457.5, and 391.7 nm, respectively, based on the absorption measurements. The latter three have been assigned tentatively to exotic $C_{11}H_9^{+}$ isomers, namely, A^+, C^+, and B^+ (Chart 1b). TD DFT calculations predict strong, singular transitions at 3.39, 3.07, and 3.48 eV (366, 404, and 356 nm, $f = 0.80$, 0.67, and 0.84) for the belonging radicals (Table S3, Supporting Information). The excitation energies are thus overestimated by ~0.8 eV for isomers A$^{\bullet}$ and B$^{\bullet}$ and by 0.3 eV for C$^{\bullet}$.

5. CONCLUDING REMARKS

Transitions of two isomers, benzotropylium (BzTr$^+$) and 2-naphthylmethylium (2-NyMe$^+$), dominate the absorption spectra recorded after deposition of $C_{11}H_9^{+}$ into neon matrices, regardless of the hydrocarbon used for ion production. The 1-methyl-naphthalene (1-MetN) precursor is not an exception; however, any distinct band that would belong to 1-naphthylmethylium (1-NyMe$^+$) should be detected at least in this case. The absorptions of BzTr$^+$ and 2-NyMe$^+$ are present also in spectra obtained using open-chain and ring−chain initial materials; this indicates that isomerization of $C_{11}H_9^{+}$ takes place in the ion source. BzTr$^+$ is the most stable structure on the potential energy surface of $C_{11}H_9^{+}$; hence, it is not surprising that the absorptions of this cation are seen in the spectra for all precursors. 1- and 2-NyMe$^+$ have similar energies in the ground state; however, distinct absorptions of only 2-NyMe$^+$ haven been observed instead of the expected 1-NyMe$^+$ for the 1-MetN precursor. Weak oscillator strengths of transitions of the latter does not fully explain this anomaly.

The 1-NyMe$^+$ cation initially formed from 1-MetN in the source rearranges producing BzTr$^+$ and 2-NyMe$^+$. The reaction pathway and transition states call for a high-level, quantum chemical exploration. Unimolecular isomerization of simple aromatics such as benzene or naphthalene has been studied earlier by experimental and theoretical methods. Hydrogen shift as well as scrambling of isotope-labeled ^{13}C carbon atoms have been observed.[47] Mechanisms were proposed to explain the automerization;[47,48] of course, more complex processes may play a significant role in discharges. The barrier for the isomerization of $C_{11}H_9^{+}$ is likely higher than optical excitations (greater than ~4.5 eV), because no photoconversion of the isomers has been observed upon UV irradiation of the matrices. BzTr$^+$ and 2-NyMe$^+$, once excited, decay radiatively.

Absorptions of three other isomers of $C_{11}H_9^{+}$, besides those of BzTr$^+$ and 2-NyMe$^+$, have been detected following deposition of the cations produced from 1-phenyl-4-penten-1-yne or a 2,4-hexadiyne + acetylene mixture. In these isomers, a benzene ring is fused with acyclic chain(s). TD DFT and CC2 calculations predict strong single transitions (f~1) in the visible for such cations and their corresponding neutrals.

The present work reveals that PAH-related compounds are readily formed from acyclic precursors. The reported electronic spectra serve as a starting point for gas-phase surveys and provide a means of direct monitoring in kinetic experiments on PAH formation.

■ ASSOCIATED CONTENT

Supporting Information. Electronic absorption spectra of phenylacetylene and naphthalene cations, scheme of considered $C_{11}H_9^{+}$ structures and their relative ground-state energy, calculated harmonic frequencies and vertical excitation energies of selected $C_{11}H_9^{+}$ and $C_{11}H_9^{\bullet}$ isomers and complete ref 23. This information is available free of charge via the Internet at http://pubs.acs.org/.

■ AUTHOR INFORMATION

Corresponding Author
j.p.maier@unibas.ch

[†]Permanent address: Institute of Physics, Polish Academy of Sciences, Al. Lotników 32−46, PL-02668 Warsaw, Poland.

■ ACKNOWLEDGMENT

This work has been financed by the *Swiss National Science Foundation* (Project No. 200020-124349/1).

REFERENCES

(1) Cox, N. L. J. In *PAHs and the Universe: A Symposium to Celebrate the 25th Anniversary of the PAH Hypothesis*; Joblin, C., Tielens, A. G. G. M., Eds.; EAS Publications Series, Vol. 46; EDP Sciences: Les Ulis, France, 2011; p 349.

(2) Tielens, A. G. G. M. In *PAHs and the Universe: A Symposium to Celebrate the 25th Anniversary of the PAH Hypothesis*; Joblin, C., Tielens, A. G. G. M., Eds.; EAS Publications Series, Vol. 46; EDP Sciences: Les Ulis, France, 2011; p 3.

(3) Waite, J. H.; Young, D. T.; Cravens, T. E.; Coates, A. J.; Crary, F. J.; Magee, B. A.; Westlake, J. *Science* **2007**, *316*, 870.

(4) Miller, J. A.; Klippenstein, S. J. *J. Phys. Chem. A* **2001**, *105*, 7254.

(5) McEnally, C. S.; Pfefferle, L. D.; Atakan, B.; Kohse-Höinghaus, K. *Prog. Energy Combust. Sci.* **2006**, *32*, 247.

(6) Richter, H.; Howard, J. B. *Prog. Energy Combust. Sci.* **2000**, *26*, 565.

(7) Bockhorn, H.; Fetting, F.; Wenz, H. W. *Ber. Bunsen-Ges. Phys. Chem.* **1983**, *87*, 1067.

(8) Frenklach, M.; Clary, D. W.; Gardiner, W. C.; Stein, S. E. *Proc. Combust. Inst.* **1984**, *20*, 887.

(9) Wang, H.; Frenklach, M. *Combust. Flame* **1997**, *110*, 173.

(10) Miller, J. A. *Proc. Combust. Inst.* **1996**, *20*, 461.

(11) D'Anna, A.; Violi, A.; D'Allessio, A. *Combust. Flame* **2000**, *121*, 418.

(12) Marinov, N. M.; Pitz, W. J.; Westbrook, C. K.; Lutz, A. E.; Vincentore, A. M.; Senkan, S. M. *Proc. Combust. Sci.* **1998**, *27*, 605.

(13) Appel, J.; Bockhorn, H.; Frenklach, M. *Combust. Flame* **2000**, *121*, 122.

(14) Wen, J. Z.; Thomson, M. J.; Lightstone, M. F.; Rogak, S. N. *Energy Fuels* **2006**, *20*, 547.

(15) McKinnon, J. T.; Howard, J. B. *Proc. Combust. Inst.* **1992**, *24*, 965.

(16) Ascenzi, D.; Aysina, J.; Tosi, P.; Maranzana, A.; Tonachini, G. *J. Chem. Phys.* **2010**, *133*, No. 184308.

(17) Shukla, B.; Koshi, M. *Phys. Chem. Chem. Phys.* **2010**, *12*, 2427.

(18) Garkusha, I.; Fulara, J.; Sarre, P. J.; Maier, J. P. *J. Phys. Chem. A* **2011**, *115*, 10972.

(19) Newby, J. J.; Stearns, J. A.; Liu, C.-P.; Zwier, T. S. *J. Phys. Chem. A* **2007**, *111*, 10914.

(20) Güthe, F.; Ding, H.; Pino, T.; Maier, J. P. *Chem. Phys.* **2001**, *269*, 347.

(21) Fulara, J.; Nagy, A.; Garkusha, I.; Maier, J. P. *J. Chem. Phys.* **2010**, *133*, No. 024304.

(22) Garkusha, I.; Fulara, J.; Nagy, A.; Maier, J. P. *J. Am. Chem. Soc.* **2010**, *132*, 14979.

(23) Frisch, M. J.; et al. *Gaussian 03*, Revision C.01; Gaussian, Inc.: Wallingford, CT, 2004.

(24) *Turbomole*, version 6.2, 2010; a development of University of Karlsruhe and Forschungszentrum Karlsruhe GmbH, 1989−2007, Turbomole GmbH, since 2007; available from http://www.turbomole.com.

(25) Pino, T.; Douin, S.; Boudin, N.; Bréchignac, Ph. *J. Phys. Chem. A* **2007**, *111*, 13358.

(26) Xu, H.; Johnson, P. M.; Sears, T. J. *J. Phys. Chem. A* **2006**, *110*, 7822.

(27) Boudin, N.; Pino, T.; Bréchignac, Ph. *J. Mol. Struct.* **2001**, *563*, 209.

(28) Andrews, L.; Kelsall, B. J.; Blankenship, T. A. *J. Phys. Chem.* **1982**, *86*, 2916.

(29) Salama, F.; Allamandola, L. J. *J. Chem. Phys.* **1991**, *94*, 6964.

(30) Negri, F.; Zgierski, Z. *J. Chem. Phys.* **1994**, *100*, 1387.

(31) Nagy, A.; Fulara, J.; Garkusha, I.; Maier, J. P. *Angew. Chem., Int. Ed.* **2011**, *50*, 3022.

(32) Nagy, A.; Garkusha, I.; Fulara, J.; Maier, J. P. 2011, manuscript in preparation.

(33) Forney, D.; Althaus, H.; Maier, J. P. *J. Phys. Chem.* **1987**, *91*, 6458.

(34) Mamedov, Kh. I.; Nasibov, I. K. *Opt. Spectrosc.* **1971**, *30*, 565.

(35) Chalyavi, N.; Troy, T. P.; Nakajima, M.; Gilbson, B. A.; Nauta, K.; Sharp, R. G.; Kable, S. H.; Schmidt, T. W. *J. Phys. Chem. A* **2011**, *115*, 7959.

(36) Naville, G.; Strauss, H.; Heilbronner, E. *Helv. Chim. Acta* **1960**, *43*, 1221.

(37) Doering, W. v. E.; Knox, L. H. *J. Am. Chem. Soc.* **1954**, *76*, 3203.

(38) Dewar, M. J. S.; Pettit, R. *J. Chem. Soc.* **1956**, 2021.

(39) Becke, A. D. *Phys. Rev. A* **1988**, *38*, 3098.

(40) Lee, C.; Yang, W.; Parr, R. G. *Phys. Rev. B* **1988**, *37*, 785.

(41) Burke, K.; Werschnik, J.; Gross, E. K. U. *J. Chem. Phys.* **2005**, *123*, No. 062206.

(42) Christiansen, O.; Koch, H.; Jørgensen, P. *Chem. Phys. Lett.* **1995**, *243*, 409.

(43) Hättig, C.; Weigend, F. *J. Chem. Phys.* **2000**, *113*, 5154.

(44) Stanton, J. F. *Faraday Discuss.* **2011**, *150*, 331.

(45) Fortenberry, R. C.; King, R. A.; Stanton, J. F.; Crawford, T. D. *J. Chem. Phys.* **2010**, *132*, No. 144303.

(46) Janssen, C. L.; Nielsen, I. M. B. *Chem. Phys. Lett.* **1998**, *290*, 423.

(47) Bettinger, H. F.; Schreiner, P. R.; Schaefer, H. F., III; Schleyer, P. v. R. *J. Am. Chem. Soc.* **1998**, *120*, 5741.

(48) Schwarz, H.; Bohlmann, B. *Org. Mass Spectrom.* **1973**, *7*, 23.